Materials Transactions, Vol. 54, No. 3 (2013) pp. 337 to 343

Effects of Plating Conditions on Electroless Ni–Co–P Coating Prepared from Lactate-Citrate-Ammonia Solution

Akira Toda[1], Pornthep Chivavibul[2,*] and Manabu Enoki[2]

[1]*Meltex Inc., Tokyo 103-0004, Japan*
[2]*Department of Materials Engineering, The University of Tokyo, Tokyo 113-8656, Japan*

An electroless Ni–Co–P plating solution, which composed of lactate-citrate-ammonia as buffering and complexing agents, has been prepared. Various electroless Ni–Co–P coatings were deposited from this solution to investigate the effects of ion concentrations, pH and bath temperatures on the chemical composition of the deposited coating. The results showed that the present electroless Ni–Co–P plating solution has a potential for depositing Ni–Co–P coatings with an average composition of 71 mass% Ni, 17 mass% Co and 12 mass% P. The plating solution showed a good stability to deposit the coatings with a small deviation in compositions over wide ranges of pH values in acid region, bath temperatures, cobalt-ion and hypophosphite-ion concentrations. The nickel content of the Ni–Co–P coating could be tailored by varying nickel-ion concentrations of plating bath. The Ni content increased with increasing nickel-ion concentration while the opposite trend was observed for Co content. However, plating in the alkaline region showed significant changes in coating composition and plating behavior. Systematic UV–visible absorption measurement showed the change of complex ions from acid to alkaline regions, which could explain the different plating behavior in those regions. [doi:10.2320/matertrans.M2012292]

(Received August 24, 2012; Accepted December 20, 2012; Published February 8, 2013)

Keywords: *electroless plating, nickel-cobalt-phosphorous, composition, plating condition, complex ion, UV–Vis*

1. Introduction

Electroless nickel polyalloy deposits have been developed and used widely in many fields because their physical, chemical and magnetic properties can be tailored by additional element.[1,2] For example, cobalt is considered to be the most common additional element for imparting magnetic properties in Ni–P and Ni–B alloy deposits. There are many researches about electroless Ni–Co–P alloy deposits.[3–9] These deposits are used as a thin film magnetic recording media and an electromagnetic shielding film. The magnetic properties of Ni–Co–P deposits depend on their microstructure and thickness. The microstructure of electroless Ni–Co–P deposit, in turn, depends on the chemical species present in the plating bath and the operating conditions employed.[4]

Most of the Ni–Co–P deposits are produced from alkaline bath where the deposition rate is high (15–20 μm/h). Consequently the metal and the reducing agent in the bath are highly consumed and the pH decreases. In order to keep the process stable, the bath composition and condition have to be maintained. Ammonium hydroxide is commonly added to restore the pH value of the bath during plating. However, the unwanted by-product of ammonia gas yields a sharp, irritating, pungent odor, which is toxic by inhalation. Therefore, the enough air ventilation is required. In this study, the electroless Ni–Co–P plating solution, which composed of lactate-citrate-ammonia as buffering and complexing agents, has been developed for acid bath. The suppression of ammonia gas during plating and low deposition rate are expected. The effects of ion concentrations, pH and bath temperatures of the plating bath on the chemical composition of the deposited coatings were investigated to verify the performance of the present solution. UV–visible absorption measurement was carried out to investigate the complex ion formation of the plating bath.

*Corresponding author, E-mail: pornthep@rme.mm.t.u-tokyo.ac.jp

2. Experimental Procedure

2.1 Electroless plating procedures

Commercially available copper sheet with a thickness of 0.3 mm was used as the substrate for electroless Ni–Co–P coating deposition. Electroless plating was carried out by Meltex Inc. A series of pre-treatment steps were required to ensure good quality deposits. The pre-treatment series started with electrolytic degreasing using alkali-based solution (Cleaner-160) at 338 K followed by acid dipping using fluoride-based solution (ENTHACID-82N) for 30 s at room temperature. Next, the specimens were surface activated by dipping in a mixed solution (Melplated Activator 352 + 35 vol% HCl) for 60 s at room temperature to let substrate surface be deposited with Pd metal for triggering the reaction of Ni–Co–P deposition. After each step, the substrate was rinsed with deionized water. After pre-treatment the substrate was immediately dipped in an electroless plating bath for the deposition of Ni–Co–P coating. The standard bath composition and plating condition are listed in Table 1, where sodium hypophosphite was used as reducing agent, sodium lactate and ammonium citrate were used as complexing and buffering agents, cobalt sulfate and nickel sulfate were the sources of Co^{2+} and Ni^{2+} ions, respectively, the pH value of the bath was adjusted with dilute NaOH and H_2SO_4, the plating temperature of 353 K was kept constant along plating process.

2.2 Examination of effect of plating parameters

In order to examine the effect of ion concentration, the concentration of cobalt sulfate, nickel sulfate and sodium hypophosphite were varied from standard condition by half and a factor of two. The effects of pH value and temperature were also studied. The temperature was varied from 343 to

Table 1 Bath compositions and operation condition for Ni–Co–P electroless plating at standard condition.

Co source	$CoSO_4 \cdot 7H_2O$	1.0×10^{-1} mol·dm^{-3}
Ni source	$NiSO_4 \cdot 6H_2O$	0.87×10^{-1} mol·dm^{-3}
Reducing agent, P source	$NaH_2PO_2 \cdot H_2O$	2.8×10^{-1} mol·dm^{-3}
Buffering and complexing agents	Tri-Ammonium Citrate	2.1×10^{-1} mol·dm^{-3}
	50%-Sodium lactate Solution	7.0×10^{-1} mol·dm^{-3}
pH adjusting	H_2SO_4 + NaOH	6
Temperature, T/K		353

Table 2 Solution compositions for UV–vis spectroscopy.

Chemical solution	Solution volume for each measurement condition (ml)								
	(1)	(2)	(3)	(4)	(5)	(6)	(7)	(8)	(9)
$NiSO_4 \cdot 6H_2O$ (1.0 mol·dm^{-3})	8.8	8.8	8.8	8.8					8.8
$CoSO_4 \cdot 7H_2O$ (1.0 mol·dm^{-3})					10	10	10	10	10
50%-Sodium lactate (1.0 mol·dm^{-3})	70				70				70
Tri-Sodium citrate dehydrate (1.0 mol·dm^{-3})		21				21			
Ammonium sulphate (1.0 mol·dm^{-3})			60				60		
Tri-ammonia citrate (1.0 mol·dm^{-3})				21				21	21

363 K and the pH value was varied from 5.5 to 9. Noted that there is only one variable while the others were as listed in the standard condition. The thickness of Ni–Co–P coatings deposited from all conditions was approximately 1 μm.

2.3 Evaluation of complex ions

UV–visible spectrum measurement was conducted to study the status of nickel and cobalt complexes in the solution. In order to examine the effects pH on complex ion formation, various solutions as shown in Table 2 were prepared and the pH values of each solution were adjusted to 5, 6.5 and 8 by adding dilute NaOH and H_2SO_4. The absorbance at wavelengths from 250 to 850 nm was measured at room temperature.

2.4 Coating characterization

The cross-sections of the coatings were obtained by embedding specimens in cold mounting resin followed by grinding and polishing to a 1 μm finish and examined by scanning electron microscope (SEM). The chemical compositions of the coatings were analyzed by energy dispersive X-ray (EDX) spectrometer. A transmission electron microscope was used to observe detailed microstructure in plain view and obtain diffraction pattern of electroless Ni–Co–P coatings.

3. Results

3.1 Phase structure and morphology

BSE image of polished cross-section of Ni–Co–P coating deposited at standard condition is shown in Fig. 1(a). It reveals that the coating was dense and its thickness was uniform over the specimen surface. The coating surface was smooth and flat. TEM in-plane view and diffraction pattern of Ni–Co–P coatings deposited at standard condition are shown in Fig. 1(b). The diffraction pattern displays two broad rings indicating that the structure of Ni–Co–P coating is a mixture of nano-sized crystallite and amorphous. These inner and outer broad peaks are attributed to Ni with face-centered cubic structure and Co with close-packed hexagonal structure, respectively. TEM micrograph reveals many black clusters with the sizes under 20 nm.

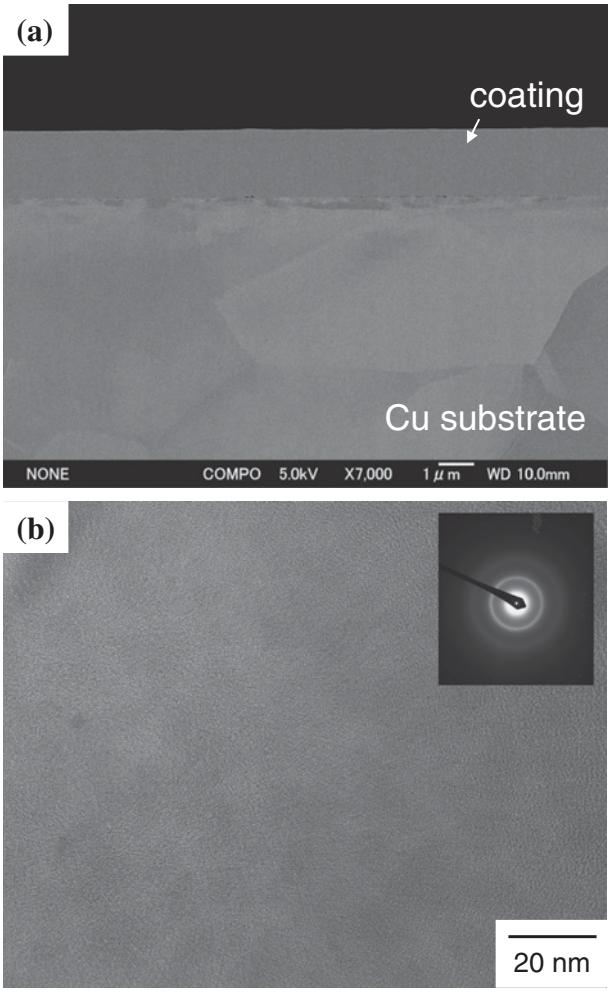

Fig. 1 Observation of Ni–Co–P coating deposited at standard condition: (a) BSE image of polished cross section, (b) TEM in-plane view with diffraction pattern.

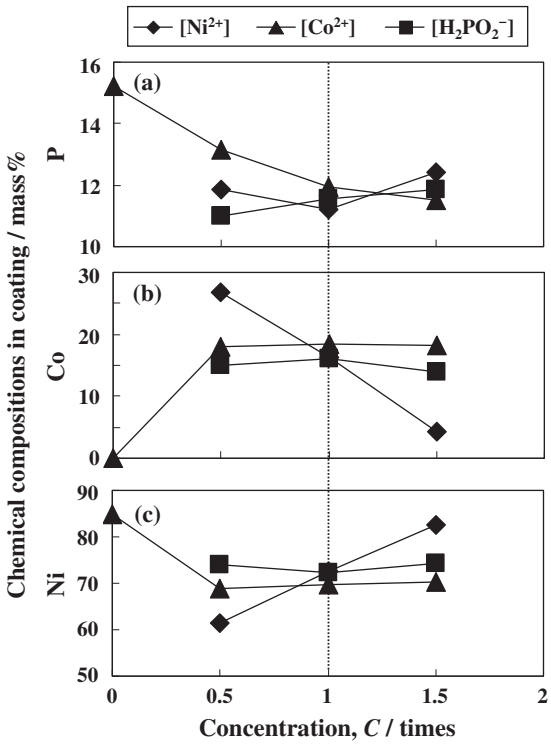

Fig. 2 Effects of ion concentrations of plating bath on coating composition.

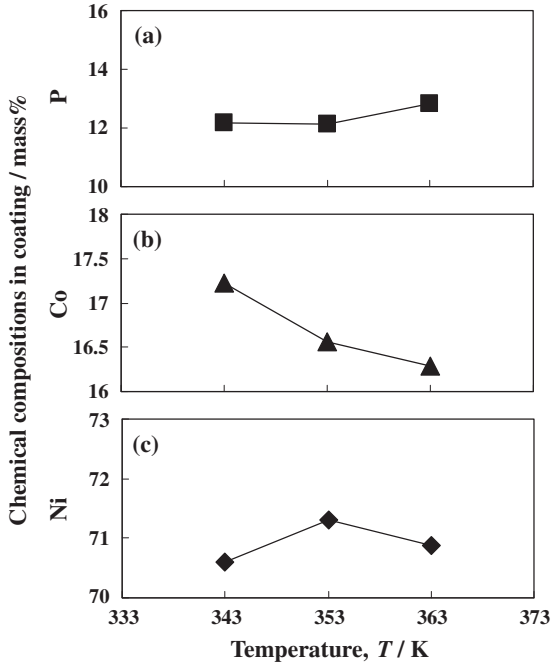

Fig. 3 Effect of temperature of plating bath on coating composition.

3.2 Effect of ion concentration on chemical composition of Ni–Co–P coatings

Figure 2 shows plots of ion concentrations in plating bath and chemical composition of Ni–Co–P coatings. The chemical composition of the coatings shown in the plots was measured by EDX and the ion concentration was varied from standard condition by half and a factor of two. The P content in the coating tended to reduce with increasing $[Co^{2+}]$ concentration in the bath, while no significant change of P content was observed with varying $[Ni^{2+}]$ and $[H_2PO_2^-]$ concentrations (Fig. 2(a)). Except for $[Co^{2+}] = 0$, which Ni–P coating was deposited, the P contents in the Ni–Co–P coatings ranged from 11 to 13 mass% for all ion concentrations. Since this deviation was small, it can infer that there is no effect of ion concentration on the P content of the Ni–Co–P coatings. Considered Ni and Co contents (Figs. 2(b) and 2(c)), there were no significant changes of Ni and Co contents with varying $[Co^{2+}]$ and $[H_2PO_2^-]$ concentrations (excluding for $[Co^{2+}] = 0$). On the other hand, the $[Ni^{2+}]$ concentration strongly influenced Ni and Co contents, where Ni content increased with increasing $[Ni^{2+}]$ concentrations and the opposite trend was observed for Co content.

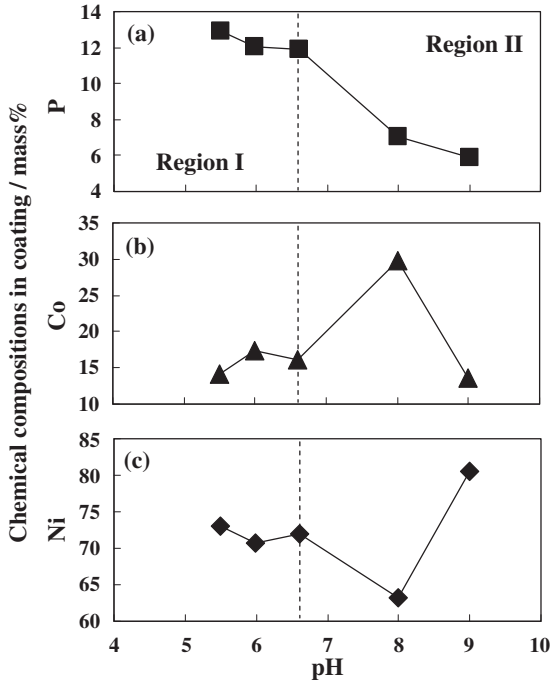

Fig. 4 Effect of pH of plating bath on coating composition.

3.3 Effects of temperature and pH on chemical composition of Ni–Co–P coatings

Figure 3 shows the effect of bath temperature on the chemical composition of Ni–Co–P coatings. Increasing bath temperature from 343 to 363 K, there were small changes of approximately 1 mass% for P and Ni contents (Figs. 3(a) and 3(b)). The Co content tended to reduce with increasing bath temperature, however, a reduction was small (∼1 mass%). Therefore, it can infer that bath temperature do not influence chemical composition of the coating for the present plating bath. Effect of pH on the chemical composition of Ni–Co–P coatings is shown in Fig. 4. There were two regions which could be identified, i.e., acid (pH < ∼6.6) and alkaline (pH > ∼6.6) regions. In the first region, no significant changes of all compositions with varying pH values were observed. However, dramatic changes of all compositions were observed in the latter region. The P content significantly reduced and unidentified relationship between Ni and Co contents with pH values was observed.

3.4 Deposition rate

Figure 5(a) shows the relationship of deposition rate versus ion concentrations. The deposition rate of Ni–P ($[Co^{2+}] = 0$) was the lowest one, while the deposition rate slightly decreased with increasing $[Co^{2+}]$ concentration. Varying $[H_2PO_2^-]$ concentration seemed to have no influence on deposition rate. A linear increase of deposition rate with $[Ni^{2+}]$ concentration was observed. The deposition rate also increased with increasing bath temperature as shown in Fig. 5(b).

The effect of pH on the deposition rate is shown in Fig. 5(c). It could be divided into two regions, i.e., acid and alkaline regions as observed in Fig. 4. In the first region, no significant change of deposition rate with varying pH value was observed. However, dramatic increase of deposition rate with pH value was observed in the latter region.

3.5 UV–visible spectrum measurement

Figure 6 shows UV–vis spectrums of the $NiSO_4$, $CoSO_4$ aqueous solutions with addition of various complexing agents as listed in Table 2 at pH values of 5 to 8. The spectrums of the pure $NiSO_4$ and $CoSO_4$ aqueous solutions are also given for a comparison and their first peaks were at 394 and 511 nm, respectively. With the addition of sodium lactate (solutions (1) and (5)), the peak positions of Ni and Co moved to 392 and 524 nm, respectively (Fig. 6(a)). This meant that there were formations of Ni-lactate and Co-lactate complex ions. One point should be noted that the intensities of both Ni-lactate and Co-lactate spectrums were almost the same for all pH values (acid to alkaline solutions), this could infer that pH had no effect on the lactate complex formation. Moreover, when the experiment time proceeded, solid precipitation was observed in Co solutions (solution (5)) with pH values of 5 and 6.5. This meant that the Co-lactate complex ion is not stable in acid region. With the addition of sodium citrate (solutions (2) and (6)), the peak positions of Ni for all pH values moved to 384 nm with the same intensities showing the formation of Ni-citrate complex ion (Fig. 6(b)). However, those of Co moved to 508 and 530 nm for acid (pH 5, 6.5) and alkaline (pH 8) solutions, respectively. These meant that while there was only one type of Ni-citrate complex ion, two types of Co-citrate complex ions were formed depending on the pH value. The Co-citrate complex formed in alkaline solution seemed to be less stable than those formed in acid solution due to its higher wave length. Figure 6(c) shows the spectrums of Ni-ammonia (solution (3)) and Co-ammonia (solution (7)) complex ions. Noted that the measurement could not be made at the pH values of 5 and 6.5 because of the $Ni(OH)_2$ and $Co(OH)_2$ precipitation during pH adjustment. The Ni and Co peaks shifted to 377 and 508 nm, respectively, implying that the formation of both Ni-ammonia and Co-ammonia complex ions can take place only in the alkaline solution. Figure 6(d) showed spectrums when adding tri-ammonia citrate solutions (solutions (4) and (8)). The Ni peaks shifted to 384 and 382 nm, for acid (pH 5, 6.5) and for alkaline (pH 8) solutions, respectively. Since the spectrum peaks in acid region were the same as those observed in solution with sodium citrate (Fig. 6(b)), these peaks were likely for Ni-citrate complex ion. At pH of 8, spectrum peak located between spectrums of Ni-citrate (384 nm) and Ni-ammonia (377 nm) complexes, therefore, this peak can be considered to Ni-citrate-ammonia complex. The similar behavior was also observed for Co, i.e., the Co-citrate peaks (508 nm) were detected in acid solution and Co-citrate-ammonia peak (526 nm), which located between spectrums of Co-citrate (530 nm, pH 8) and Co-ammonia (508 nm, pH 8) was observed for alkaline solution. The spectrums of complex ions in plating solution (solution (9)) are given in Fig. 6(e). The Ni peaks shifted to 389 and 390 nm for acid (pH 5, 6.5) and alkaline (pH 8) solutions. Since these peaks located between Ni-lactate and Ni-citrate/Ni-ammonia peaks, it can be considered that these peaks were from Ni-lactate-citrate and/or Ni-lactate-citrate-ammonia complex ions. The Co peaks shifted to 513, 518 and 534 nm for pH values of 5, 6.5 and 8, respectively. In the acid region, Co peaks were between the peaks of Co-citrate (508 nm) and Co-lactate (524 nm) showing the formation of Co-lactate-citrate complex ions. However, the Co peak at pH of 8 shifted to higher wavelength than those observed for other complex ions. This behavior is unexpected pointing out that there is a new formation of Co complex. One point should be noted that the intensities of both Ni and Co complexes spectrums in acid solution were almost the same, while those measured at pH of 8 showed higher intensities. This could infer that alkaline bath had strong effect on the complex ion formation of plating solution.

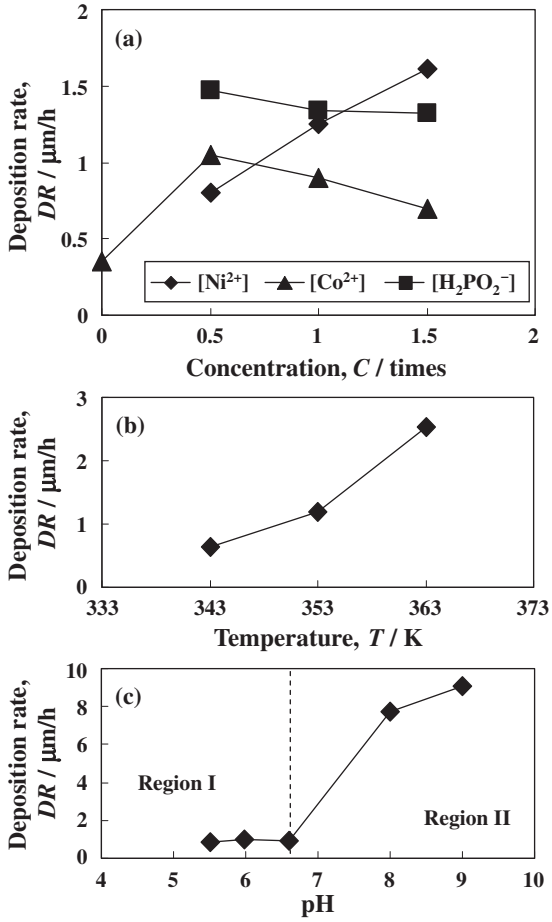

Fig. 5 Deposition rate as a function of (a) ion concentrations, (b) temperature and (c) pH.

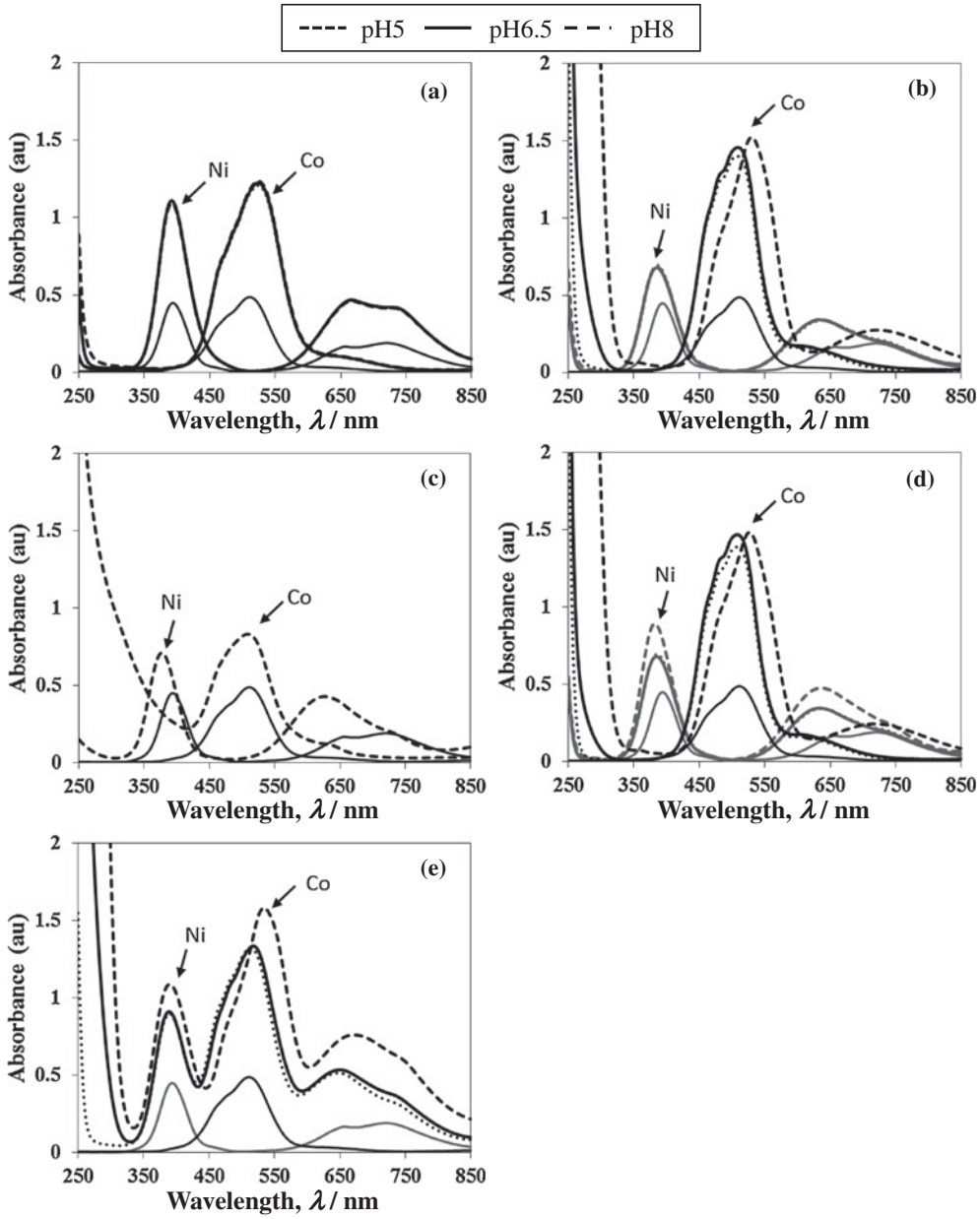

Fig. 6 The UV–vis spectra of nickel and cobalt solution at several pH values with the addition of (a) sodium lactate, (b) sodium citrate, (c) ammonia sulphate, (d) ammonia citrate and (e) plating solution.

4. Discussion

The present study has shown that the average chemical composition of Ni–Co–P coating plated at standard condition composed of 71 mass% Ni, 17 mass% Co and 12 mass% P and these values were stable over various plating conditions. Varying $[Co^{2+}]$ and $[H_2PO_2^-]$ concentrations from 0.5 to 2 times of those at standard condition, pH values from 5.5 to 6.6 and bath temperatures from 343 to 363 K were found to have no influence on the chemical composition of the coating. While the Ni and Co contents of the coating can be tailored by adjusting the $[Ni^{2+}]$ concentration. Therefore, it can deduce that the bath composition of the present study is appropriate for deposit the Ni–Co–P coating with an average 12 mass% P.

Generally, the oxidizing and reducing reactions occurring during electroless Ni–Co–P plating[10] can be represented as below

$$H_2PO_2^- + H_2O \rightarrow H_2PO_3^- + 2H, \quad (1)$$

$$H_2PO_2^- + H \rightarrow P + OH^- + H_2O, \quad (2)$$

$$2H \rightarrow H_2\uparrow, \quad \Delta G^\circ = 0.0\,\text{kJ} \quad (3)$$

$$Ni^{2+} + 2H \rightarrow Ni + 2H^+, \quad (4)$$

$$Co^{2+} + 2H \rightarrow Co + 2H^+. \quad (5)$$

Firstly, the Pd-nuclei at the Cu surface stimulate reaction (1) to take place yielding the hydrogen atoms. These hydrogen atoms reduce nickel ions yielding the deposition of Ni at the Cu surfaces (reaction (4)). Since Ni is also catalytic active as same as Pd, as soon as Ni metal atoms are deposited the reaction (1) continuously takes place providing the high concentration of hydrogen atom and the reduction of Ni^{2+} ions afterward becomes self-sustainable. These generated hydrogen atoms further reduce $H_2PO_2^-$ ions and Co^{2+} ions as shown in reactions (2) and (5), respectively and some are

combined to generate hydrogen gas (reaction (3)). Cobalt is also catalytic active as similar as Pd and Ni, therefore the reaction (1) should take place even nickel is absent. However, there was no deposition of cobalt at Cu surfaces when $[Ni^{2+}] = 0$. This means that the Co cannot act as an active catalyst at the present plating condition (pH = 6, $T = 353$ K). According to this finding, it can infer that the deposition of Co in the coating cannot exclusively occur without the deposition of Ni for the present plating bath. The same behavior is also expected for the deposition of P. The deposition of the Ni is a key factor to the entire coating process and influence the coating composition for the present plating bath. As described in the sections 3.2 and 3.4, the Ni content in the coating and deposition rate increased with $[Ni^{2+}]$ concentration while there was no change in chemical composition of the coating and deposition rate with varying $[Co^{2+}]$ and $[H_2PO_2^-]$ concentrations. These evidences supported that the deposition of the coating is controlled by Ni.

Generally, temperature has a considerable effect on the rate of process. The rate of process increases with increase in temperature. The results from the present study showed the same behavior (Fig. 4(b)). The deposition rate increased about twice with an increase in temperature of 10 K. The pH values also have a strong effect on the electroless plating. It is wildly known that increasing pH the deposition rate increases and phosphate solubility decreases. The effect of pH on the coating composition and deposition rate in the present study could be divided into two regions as described previously, i.e., acid and alkaline regions. In the acid region, there were no significant changes of both coating composition and deposition rate. On the other hand, the deposition rate dramatically increased and the phosphorous content in the coating decreased in the alkaline region. Possible explanations for this behavior are as followings. In the alkaline solution, the oxidation of hypophosphite reaction occurs as follow:

$$H_2PO_2^- + 3OH^- \rightarrow HPO_3^{2-} + 2H_2O. \quad (6)$$

From the above chemical reaction, an increase in pH value (OH^- ion concentration) leads to increasing in oxidation rate of hypophosphite. Moreover, there is a report that the rate of electroless cobalt plating is acceptable only at pH > 7.[11] This means that while only the autocatalytic reaction of nickel takes place in the acid solution, both of nickel and cobalt take place in the alkaline solution. It is reasonable that these reactions accelerate the deposition rate yielding higher deposition rate in alkaline region. The effects of pH on cobalt and nickel contents in the coating in the alkaline region (Figs. 4(b) and 4(c)) in the present study were similar as those observed by Kim *et al.*,[3] i.e., Ni content decreased in the pH region from 7.0 to 8.0 and then the Ni content increased with rising pH. The opposite trend was observed for Co content. They suggested that this might be due to formation of different complexes at the different operating conditions.

UV–vis spectrum results revealed useful information to explain the plating behavior of the present study. There are nine types of ions in the present plating bath. Among these ions, H^+, Na^+, and SO_4^{2-} (the two latter ones were from pH adjusting agent) ions seem to have no effects on the coating composition. The Ni^{2+} and Co^{2+} ions combine with lactate ($C_3H_5O_3^-$), citrate ($C_6H_5O_7^{3-}$) and ammonium (NH_4^+) ions to form complex ions. The complex formation strongly depends on pH value as described in section 3.5. The acidity constant (pK_a) of lactate is 3.79 and those of citrate are 3.09, 4.75 and 6.4 for pK_{a1}, pK_{a2} and pK_{a3}, respectively. According to these values, most of lactate molecules are in the form of ion in the plating solution while some of citrate ions interact with hydrogen ions to form intermediate ions of hydrogen citrate ($HC_6H_5O_7^{2-}$) and dihydrogen citrate ($H_2C_6H_5O_7^-$) when pH value becomes higher. Based on the UV–vis spectrum results as shown in section 3.5, the complex ion formation behavior can be mainly divided into two regions; acid and alkaline regions. The pH value had small effect on the complex formation of both Ni and Co in acid region. In contrast, dramatic change in complex ion formation behavior, especially for Co was observed in the alkaline region. The formations of Ni-lactate and Ni-citrate complex ions seemed to be unaffected with pH value because no peak shifts and intensity change were observed (Figs. 6(a), 6(b)). The same behavior was also observed for Co-lactate complex (Fig. 6(a)), however Co-citrate complex formation significantly changed in alkaline regions (Fig. 6(b)). The large peak shift was observed. The ammonium ion seemed to influence the complex ion formation only in alkaline region. This could be clearly seen from peak shifts observed in Na_3citrate (Fig. 6(b)) and $(NH_4)_3$citrate (Fig. 6(d)) solutions at pH of 8 while no peak shifts were observed in acid region. The peaks of Ni in Na_3citrate and $(NH_4)_3$citrate solutions located at 384 and 382 nm, respectively and those for Co located at 530 and 526 nm, respectively. Those peaks observed in $(NH_4)_3$citrate solutions shifted into the shorter wavelength (toward Ni/Co-ammonia complex peak) and were for Ni/Co-citrate-ammonia complexes. Based the experiment observation, the ammonia gas generated only when the pH > 8 implying that the reduction of ammonium ion could take place in alkaline region. Considering the plating solution (Fig. 6(e)) where various ions are concerned, the peak shift and intensity change were not observed for Ni in acid region while in alkaline region both peak shift and intensity change were identified showing that the effect of other ions such as ammonia and citrate. The similar behavior was also observed for Co, but the peak shift and intensity change were outstanding. These findings can explain the variation of chemical composition of the deposit prepared from acid and alkaline bath (Fig. 4). The constant chemical composition of the deposits prepared from the acid bath originated from the stable complex ion over a range of pH while the change of complex ion with pH in alkaline region yielded the fluctuation in chemical composition. The Co complex became active and the effect of ammonia on the complex ion formation play an important role in plating process. Contrast to the present work, which the plating solution was designed for acid bath, most of research works,[3,4,12,13] which make a deposition of Ni–Co–P coatings in alkaline bath added ammonium chloride (NH_4Cl) or ammonium sulfate ($(NH_4)_2SO_4$) as a buffering agent to balance the ammonia ion in the plating bath.

5. Conclusions

(1) It has been shown that the present electroless Ni–Co–P plating solution has a potential for depositing Ni–Co–P coatings with an average composition of 71 mass% Ni, 17 mass% Co and 12 mass% P. The developed solution shows a good stability over the pH values of 5.5 to 6.6, bath temperatures of 343 to 363 K, $[Co^{2+}]$ and $[H_2PO_2^-]$ concentrations of 0.5 to 2 times of those at standard condition.

(2) The Ni content of the Ni–Co–P coating can be tailored by varying $[Ni^{2+}]$ concentrations of plating bath. The Ni content increases with increasing $[Ni^{2+}]$ concentration while the opposite trend is observed for Co content. The deposition rate of the coating can be raised by increasing bath temperature.

(3) The Ni deposition is the key factor to control the plating process in acid region and chemical composition of the coating in the present plating bath with acidic solutions. The deposition of Co and P cannot be occurred without the deposition of Ni.

(4) The different plating behavior in acid and alkaline regions originated from the change of complex ions. The Ni and Co complexes were stable in acid region, while in alkaline region the Co complex formation changed and the effect of ammonia ion became pronounced.

REFERENCES

1) G. O. Mallory and T. R. Horhn: Plat. Surf. Finish. **66** (1979) 40–46.
2) J. Li, X. G. Hu and D. L. Wang: Plat. Surf. Finish. **83** (1996) 62–64.
3) D. H. Kim, K. Aoki and O. Takano: J. Electrochem. Soc. **142** (1995) 3763–3767.
4) T. Sankara Narayanan, S. Selvakumar and A. Stephen: Surf. Coat. Technol. **172** (2003) 298–307.
5) D. N. Lee and K. H. Hur: Scr. Mater. **40** (1999) 1333–1339.
6) A. A. Aal, A. Shaaban and Z. A. Hamid: Appl. Surf. Sci. **254** (2008) 1966–1971.
7) P. Chivavibul, M. Enoki, S. Konda, Y. Inada, T. Tomizawa and A. Toda: J. Magn. Magn. Mater. **323** (2011) 306–310.
8) Y. Huang, K. Shi, Z. Liao, Y. Wang, L. Wang and F. Zhu: Mater. Lett. **61** (2007) 1742–1746.
9) Y. Li, R. Wang, F. Qi and C. Wang: Appl. Surf. Sci. **254** (2008) 4708–4715.
10) G. O. Mallory and J. B. Hajdu (ed.): *Electroless Plating Fundamentals and Applications*, (The American Electroplaters and Surface Finishers Society, Florida, 1990) p. 539.
11) N. Petrov, Y. Sverdlov and Y. Shacham-Diamand: J. Electrochem. Soc. **149** (2002) C187–C194.
12) Y. Gao, L. Huang, Z. J. Zheng, H. Li and M. Zhu: Appl. Surf. Sci. **253** (2007) 9470–9475.
13) Z. B. Li, B. Shen, Y. D. Deng, L. Liu and W. B. Hua: Appl. Surf. Sci. **255** (2009) 4542–4546.